ISSN 2316-6886
WRIM

Water Resources and Irrigation Management
v.15, n.1-3, p.95-111, 2026
DOI: 10.19149/wrim.v15i1-3.5369

Cruz das Almas, BA, Brazil – https://www3.ufrb.edu.br/seer/index.php/wrim/index

---

ORIGINAL PAPER

Mitigation of salt stress by exogenous application of melatonin and its effects on physiological and biochemical aspects in soybean

Pablo Henrique de Almeida Oliveira[1], Gisele Lopes dos Santos[1], João Everthon da Silva Ribeiro[1*], Elania Freire da Silva[1], Ester dos Santos Coêlho[1], Antonio Gideilson Correia da Silva[1], José Travassos dos Santos Júnior[1], John Victor Lucas Lima[1], Ayslan do Nascimento Fernandes[1], Cícero Henrique Jacome Dantas[1], Francisco Vanies da Silva Sá[2], Aurélio Paes Barros Júnior[1] & Lindomar Maria da Silveira[1]

[1]Federal University of the Semi-Arid Region, Mossoró, Rio Grande do Norte, Brazil
[2]State University of Paraíba, Catolé do Rocha, Paraíba, Brazil

Abstract: Salinity is an abiotic stress that impairs photosynthesis and plant growth. Melatonin mitigates these effects through its cellular and physiological functions, including improving photosynthetic performance. Soybean, highly important for food security and the economy, requires strategies to reduce these impacts and to clarify its tolerance mechanisms. This research aims to explore the effects of exogenous melatonin application on gas exchange, chlorophyll a fluorescence, and biochemical characteristics of soybean under saline stress conditions. Soybean plants were cultivated in an experimental area of the Federal University of the Semi-Arid Region (UFERSA), Mossoró – RN. The experiment was conducted in a randomized block design arranged in a 3 × 3 factorial scheme (three saline levels in irrigation water – 0.5, 3.0, and 5.0 dS m^{-1} and three melatonin concentrations – 0, 0.5, and 1.0 mM), with three repetitions. The saline levels altered gas exchange, chlorophyll a fluorescence, and proline content in soybean plants. Chlorophyll a fluorescence was improved up to the saline level of 3.0 dS m^{-1}, regardless of melatonin concentration, in soybean plants. The internal CO_2 concentration and the ratio of intercellular to atmospheric CO_2 were mitigated at a saline level of 5.0 dS m^{-1} with a melatonin concentration of 0.5 mM.

Keywords: *Glycine max*, salinity, photosynthesis, phytohormone.

Introduction

Salinity, a growing abiotic stress worldwide, is a significant threat to agricultural productivity. It affects approximately 20% of irrigated agricultural land and compromises the productivity of several crops (Hailu and Mehari, 2021). Resulting from both natural processes and inadequate agricultural practices, such as the excessive use of fertilizers and the expansion of irrigated areas (Ferreira et al., 2023), as well as capillary rise of water, sea

---

[*] Corresponding author: E-mail: j.everthon@hotmail.com

Editors: Mairton Gomes da Silva & Petterson Costa Conceição Silva
Received in: 05 May, 2025
Accepted in: 21 January, 2026

level rise, runoff and deposition of salts from salinized areas, in addition to climate changes that increase evaporation and reduce salt leaching, leads to the accumulation of salts in the soil (Eswar et al., 2021). The role of global climate change in exacerbating soil salinization is a significant concern, as factors such as precipitation, potential evapotranspiration, and temperature intensify this issue (Corwin, 2021). Rising levels of salinized groundwater and extreme precipitation events contribute to this, reducing the effectiveness of irrigation and drainage systems and increasing pressure on cropland (Muhammad et al., 2023). Therefore, plants exposed to salinity experience osmotic and ionic stress, which negatively affect water and nutrient absorption and cause oxidative damage to plant cells, ultimately reducing productivity and, in severe cases, leading to plant death (Arif et al., 2020).

The accumulation of sodium (Na^+) and chloride (Cl^-) ions in plant cell vacuoles causes an osmotic imbalance, reducing the absorption of water (Stavi et al., 2021). Substitution of potassium (K^+) for Na^+ in the cytosol impairs essential biochemical reactions, such as protein synthesis, as K^+ is a vital enzyme cofactor (Atta et al., 2023). Elevated osmotic pressure also reduces the availability of essential nutrients such as calcium (Ca^{2+}) and magnesium (Mg^{2+}), leading to ionic imbalance, nutrient deficiencies, and reduced plant growth (Yildiz et al., 2020). In addition, exposure to salt stress results in damage to photosynthetic complexes, particularly photosystem II (PSII), and reduces the efficiency of gas exchange and photosynthesis, causing stomatal and non-stomatal stress that decreases CO_2 assimilation (Stefanov et al., 2024).

Soybean (*Glycine max* L. Merr.) is an essential crop for global food security and plays a vital role in the agricultural economy (Zhao et al., 2021). As a significant source of plant protein and edible oil, soybeans are essential for human and animal feed, and for a variety of industrial applications (Sharmin et al., 2020). However, sustainable soybean production faces significant challenges due to its susceptibility to abiotic stresses, such as salinity, drought, extreme temperatures, and soil nutrient deficiencies (Jahan et al., 2023), which cause substantial losses in soybean production in several regions of the world (Cotrim et al., 2021).

The hormonal stability of plants can be severely compromised by abiotic stress (Muhammad et al., 2023). In this context, melatonin, a hormone widely recognized for its antioxidant and growth-regulating functions, has shown promising results in mitigating the negative effects of these stresses (Pan et al., 2023). Studies have shown that exogenous application of melatonin in plants can increase tolerance to salt and water stress, promote hormonal balance, and improve plant resistance (Raza et al., 2023; Ribeiro et al., 2024; Coêlho et al., 2025).

The benefits of exogenous melatonin application for salt stress tolerance in various crops are well established. However, more knowledge is needed about the specific effects of this practice on soybeans, especially regarding their physiological and biochemical properties under saline conditions. Understanding these aspects is essential to optimizing photosynthetic efficiency and ensuring adequate gas exchange, even under salt-stress conditions. Thus, our study aimed to explore the effects of exogenous melatonin application on gas exchange, chlorophyll a fluorescence, and biochemical characteristics of soybean under salt stress conditions.

Materials and Methods

Experimental area

The experiment was conducted from November to December 2023 in an experimental area located at the Federal University of the Semi-Arid Region (UFERSA), in Mossoró, Rio Grande do Norte, Brazil (5º 12’ 28” S, 37º 19’ 04” W, and 24 m altitude). According to Köppen, the region's climate is classified as BSh, that is, hot and dry (Alvares et al., 2013). The climatic data during the experiment were collected from the automatic weather station of UFERSA (Figure 1), operated by the Brazilian National Institute of Meteorology (INMET).

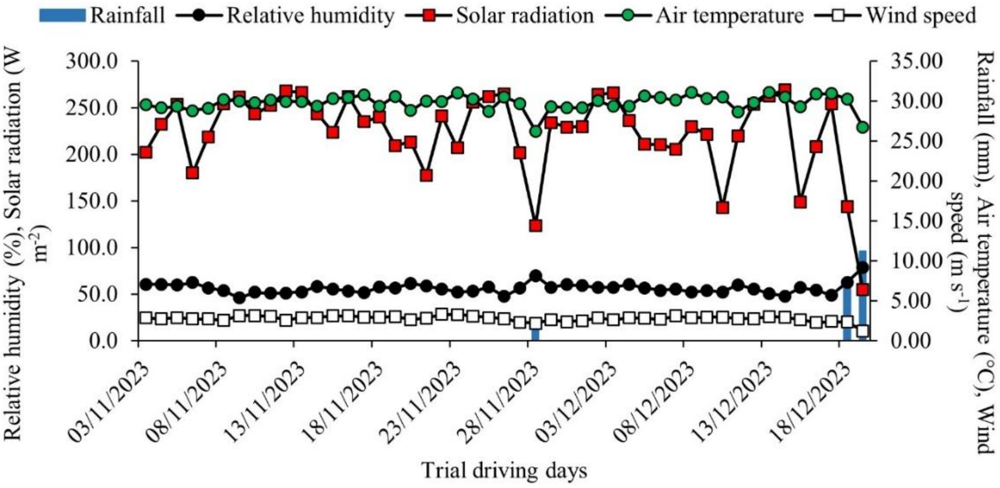

Figure 1. Average of the meteorological data during the experimental period.

Experimental design and treatments

The experimental design was in randomized blocks, arranged in a 3 × 3 factorial scheme: three levels of electrical conductivity of irrigation water – ECw (0.5, 3.0, and 5.0 dS m^{-1}) and three melatonin concentrations (0, 0.5, and 1.0 mM), with three replications. The ECw levels were set according to Oliveira et al. (2024). The salt levels were obtained by adding sodium chloride (NaCl) to the irrigation water, except for the ECw level of 0.50 dS m^{-1} (control – water supply) (Table 1). The saline solutions were prepared in 60 L plastic containers, and the amounts of NaCl were calculated according to the relationship between ECw and salt concentration (Richards, 1954). For ECw of 3.0 and 5.0 dS m^{-1}, 87.7 and 157.8 g of NaCl were used, respectively. The solutions were monitored with a CD-850 digital conductivity meter (Instrutherm Instrumentos de Medição Ltda., São Paulo, SP, Brazil) every five days to ensure stability.

Plant material and treatments

Soybean seeds (cv. Conventional Sambaíba) were sown in 2.6 L polyethylene pots, filled with local soil, classified as loamy sand (Table 2), and five seeds were sown per pot. Fertilization with nitrogen (N), phosphorus (P), and potassium (K) was carried out according to the recommendation of Gomes and Coutinho (2008), with 40 and 60 kg ha^{-1} of P_2O_5 and K_2O, respectively. Accordingly, 85 and 130 mg of P_2O_5 and K_2O were added to each pot. The sources of P and K were mono ammonium phosphate (MAP) (61% P_2O_5 and 12% N) and potassium chloride (KCl) (60% K_2O). At 7 days after sowing (DAS), thinning was performed, leaving two plants per pot. At 15 DAS, the second thinning was performed, leaving one plant per pot. The plants were irrigated daily with the water supply until the beginning of the treatments. The control of invasive plants was carried out manually whenever necessary. At 28 DAS, the plants were subjected to saline levels.

The saline treatments were applied daily, starting from the first application of melatonin. Irrigation was carried out using the weighing lysimeter method, in which the volume of water evaporated and transpired over 24 h was monitored to maintain soil moisture at 80% of field capacity, as described by Girardi et al. (2016). The melatonin solutions were prepared by dissolving in distilled water to a volume of 0.5 L and were applied weekly, totaling three applications (28, 35, and 42 DAS). The leaves were sprayed with a portable spray bottle. At melatonin concentrations, polysorbate 80 surfactant (Tween-80, 0.05% v/v) was added to increase adhesion on the leaf.

Table 1. Chemical attributes of the water supply used in irrigation in the experiment.

pH	EC	K^+	Na^+	Ca^{2+}	Mg^{2+}	Cl^-	CO_3^{2-}	HCO_3^-	C	A	SAR	H
	(dS m^{-1})	---------------------------------(mmol$_c$ L^{-1})--------------------------------									(mmol $L^{-1})^{0.5}$	(mg L^{-1})
8.8	0.50	0.25	4.23	0.70	1.90	3.00	0.60	2.80	7.08	6.40	3.7	130

pH – hydrogen potential; EC – electrical conductivity; K^+ – potassium; Na^+ – sodium; Ca^{2+} – calcium; Mg^{2+} – magnesium; Cl^- – chloride; CO_3^{2-} – carbonate; HCO_3^- – bicarbonate; C – cations; A – anions; SAR – sodium adsorption ratio $\{SAR = Na^+/[(Ca^{2+} + Mg^{2+})/2]^{0.5}\}$; H – hardness.

Table 2. Physical and chemical analysis of the soil used in the experiment (0-0.20 m depth).

pH (H_2O)	ECse	P	K^+	Na^+	Ca^{2+}	Mg^{2+}	Al^{3+}	SB	t	T	V	m	ESP
(1:2.5)	(dS m^{-1})	----(mg dm^{-3})-------			--------------(cmol$_c$ dm^{-3})-----------						-------------(%)---------		
7.11	0.06	104.7	177.4	16.4	3.20	1.10	0	4.83	4.83	4.83	100	0	1

Granulometric fractions					Textural class
---------------------------------------(kg kg^{-1})-----------------------------------					
Coarse sand	Thin sand	Total sand	Silt	Clay	
0.48	0.33	0.81	0.14	0.05	Loamy sand

pH – hydrogen potential; ECse – electrical conductivity of soil saturation extract; P, K^+, and Na^+ – phosphorus, potassium, and sodium were extracted with Mehlich 1 solution; Ca^{2+}, Mg^{2+}, and Al^{3+} – calcium, magnesium, and exchangeable aluminum were extracted with 1 M KCl solution; SB – sum of bases; t – effective cation exchange capacity; T – cation exchange capacity; V – base saturation; m – aluminum saturation; ESP – percentage of exchangeable sodium.

Variables analyzed

At 44 DAS, gas exchange and chlorophyll a fluorescence were evaluated. Gas exchange analyses were performed from 8:00 to 10:00 a.m. using an infrared gas analyzer (IRGA) model LI-6400XT (LI-COR® Biosciences, Lincoln, NE, USA). The measurements were carried out on healthy leaves, free from damage, pests, or diseases, and fully expanded in the middle third of the plants, with four leaves per plant being analyzed. The following measurement protocol was used in the IRGA chamber: relative humidity, 50-60%; airflow, 300 µmol s^{-1}; CO_2 concentration, 400 µmol mol^{-1}; and artificial light sensor area in the leaf chamber, 2 cm^2.

The following variables were measured: net CO_2 assimilation rate (A) (µmol CO_2 m^{-2} s^{-1}), stomatal conductance (gs) (mol m^{-2} s^{-1}), transpiration rate (E) (mmol H_2O m^{-2} s^{-1}), internal CO_2 concentration (Ci) (µmol CO_2 mol^{-1}), relationship between intercellular and atmospheric CO_2 concentration (Ci/Ca), and vapor pressure deficit (VPD) (kPa).

Chlorophyll a fluorescence analysis was performed using a fluorometer model LI-6400-40 LCF (LI-COR®, Biosciences, Lincoln, NE, USA) coupled to the IRGA. Initial fluorescence (Fo'), maximum fluorescence (Fm'), variable fluorescence (Fv'), basal fluorescence (Fs), variable to initial fluorescence ratio (Fv'/F0'), potential quantum yield of PSII (Fv'/Fm'), effective quantum efficiency of PSII (ΦPSII), photochemical dissipation (qP), non-photochemical dissipation (qN), and electron transport rate (ETR) were determined in sheets subjected to a saturating flash of atypical irradiation and a pulse of light in the far red region.

In addition, at 47 DAS, the plants' leaves were collected to obtain the dry mass (DM) by drying in an oven at 65ºC until they reached a constant weight. Using leaf dry mass, total soluble sugars (TSS) were determined by the phenol-sulfuric acid method (DuBois et al., 1956), with absorbance measured at 490 nm and expressed as mg of GLU/g DM. The proline content was quantified using the acid-ninhydrin method (Bates et al., 1973), measuring the absorbance of the toluene extract at 520 nm and expressing the results in mg of Pro/g DM.

Statistical analysis

The data obtained were subjected to the Shapiro–Wilk normality test ($p \geq 0.05$) and subsequently to analysis of variance by the F-test ($p \leq 0.05$). In cases of significance, means were compared using the Tukey's test ($p \leq 0.05$). The analyses were conducted using the statistical program Sisvar 5.6 (Ferreira, 2014). Principal component analysis (PCA) and Pearson's correlation were performed in R (R Core Team, 2024) to assess relationships among variables.

Results

The electrical conductivity levels of irrigation water (ECw) significantly influenced the net CO_2 assimilation rate (A) (Figure 2A), stomatal conductance (gs) (Figure 2B), and transpiration rate (E) (Figure 2C). In contrast, the exogenous application of melatonin did not significantly affect any of these gas exchange parameters. Variables A, gs, and E decreased under saline conditions (ECw 3.0 and 5.0 dS m^{-1}), showing average reductions of 55.10, 71.47, and 70.12%, respectively, when compared to non-saline conditions (ECw 0.5 dS m^{-1}).

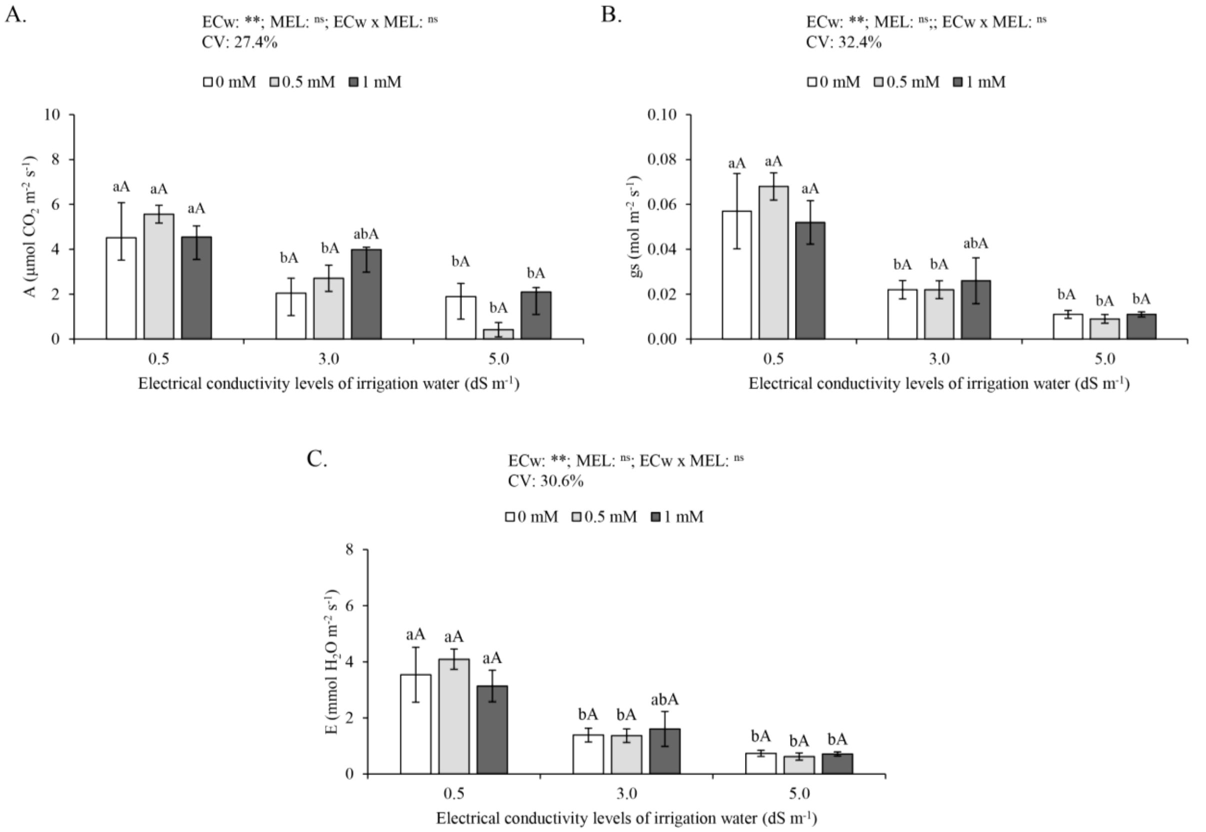

** and ns – indicate significance at $p \leq 0.01$ and not significant, respectively, according to the F-test; CV – coefficient of variation. Lowercase letters differ in electrical conductivity levels of irrigation water (ECw), and uppercase letters differ in melatonin concentrations (MEL) according to Tukey's test ($p \leq 0.05$). Vertical bars show the means ± standard deviation.

Figure 2. Net CO_2 assimilation rate – A (A), stomatal conductance – gs (B), and transpiration rate – E (C) of soybean plants subjected to different electrical conductivity levels of irrigation water and exogenous application of melatonin.

The internal CO_2 concentration (Ci) (Figure 3A), the ratio between the intercellular and atmospheric concentration of CO_2 (Ci/Ca) (Figure 3B), and vapor pressure deficit (VPD) (Figure 3C) were significantly influenced by the interaction between ECw levels and melatonin concentrations. Ci and Ci/Ca showed reductions of 82.66 and 82.64%, respectively, at ECw of 5.0 dS m^{-1} and concentration of 1.0 mM, compared to ECw of 3.0 dS m^{-1}. At ECw of 5.0 dS m^{-1}, the concentration of 0.5 mM attenuated the effects of salt stress, with increments of 82.67 and 82.64% for Ci and Ci/Ca, in the same order, when compared to the other concentrations.

The VPD increased as the salt levels intensified, with increments of 8.48, 7.04, and 11.26 % for concentrations 0, 0.5, and 1.0 mM, respectively, when compared to the 0.5 and 5.0 dS m^{-1} (Figure 3C). In addition, VPD showed a 7.18% increase in the 1.0 mM concentration compared to the 0 mM concentration.

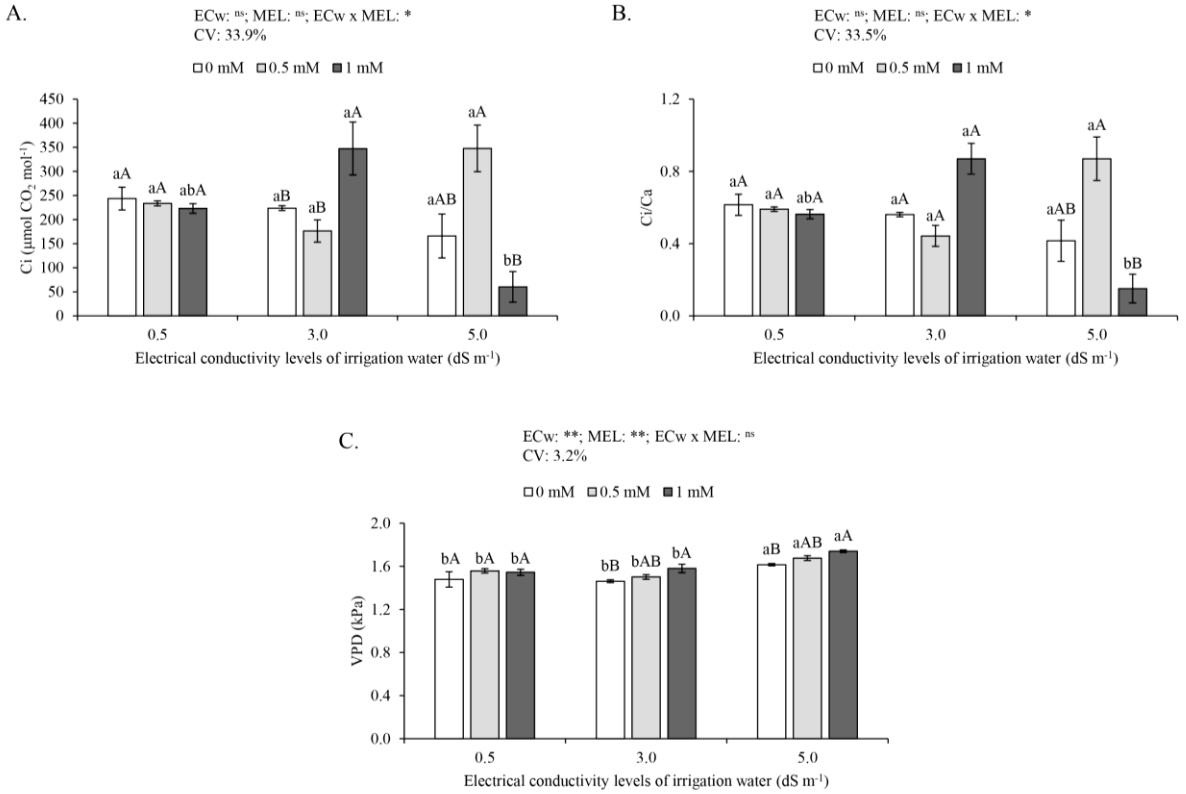

**, *, and ^{ns} – indicate significance at $p \leq 0.01$, $p \leq 0.05$, and not significant, respectively, according to the F-test; CV – coefficient of variation. Lowercase letters compare the means of electrical conductivity levels of irrigation water (ECw) within each melatonin concentration (MEL), while uppercase letters compare the means of the MEL concentrations within each ECw level by Tukey's test ($p \leq 0.05$). Vertical bars show the means ± standard deviation.

Figure 3. Internal CO_2 concentration – Ci (A), ratio between the intercellular and atmospheric concentration of CO_2 – Ci/Ca (B), and vapor pressure deficit – VPD (C) of soybean plants subjected to different electrical conductivity levels of irrigation water and exogenous application of melatonin.

The ECw significantly influenced the initial fluorescence (Fo’) (Figure 4A), maximum fluorescence (Fm’) (Figure 4B), variable fluorescence (Fv’) (Figure 4C), basal fluorescence (Fs) (Figure 4D), and the ratio between variable and initial fluorescence (Fv’/Fo’) (Figure 4E). In contrast, exogenous melatonin application did not significantly affect any of these chlorophyll *a* fluorescence variables. Variables Fo’, Fm’, Fv’, Fs, and Fv’/Fo’ decreased under saline conditions (ECw 3.0 and 5.0 dS m^{-1}), showing average reductions of 21.23, 31.13, 45.38, 27.85, and 33.48%, respectively, when compared to non-saline conditions (ECw 0.5 dS m^{-1}).

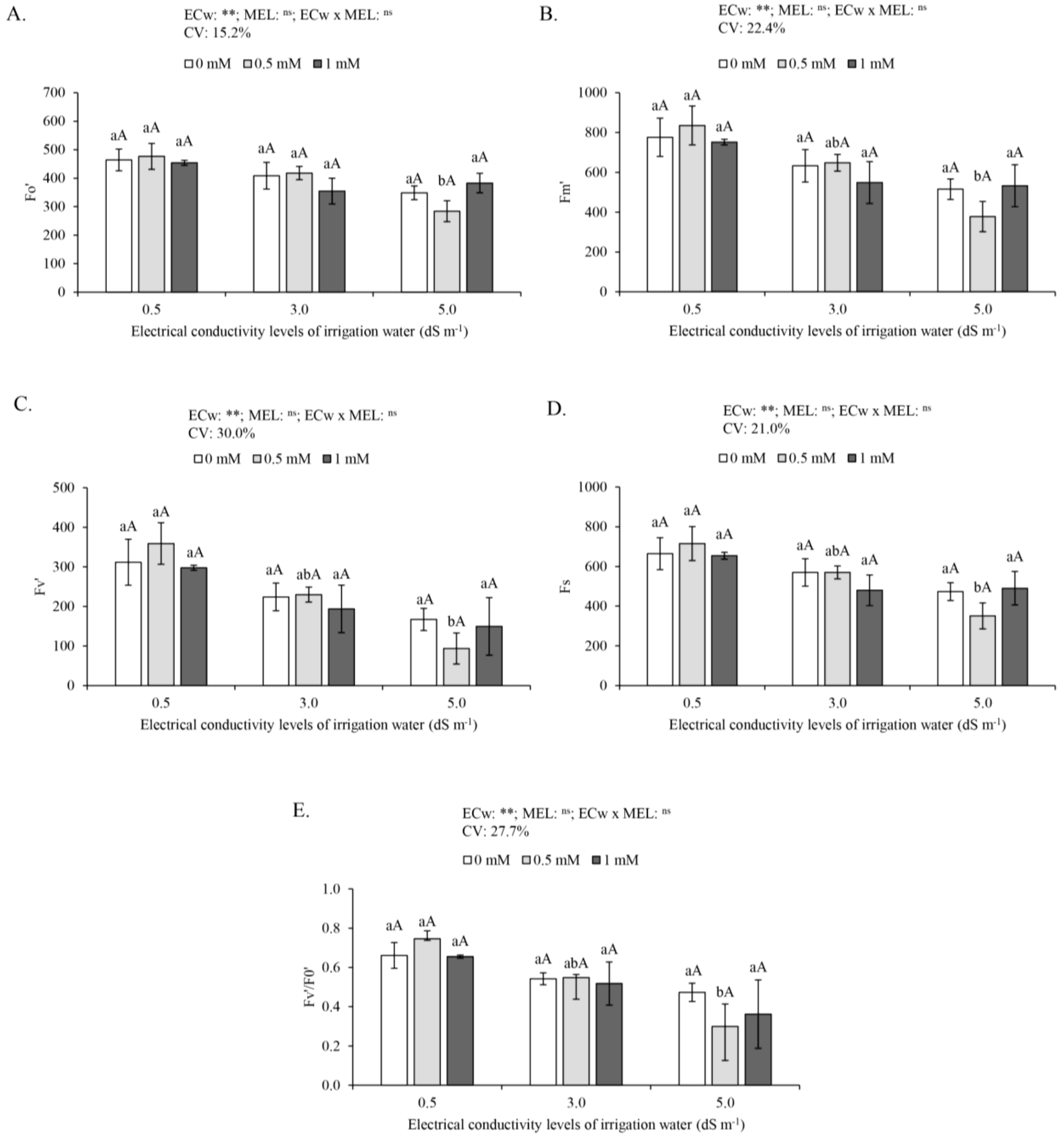

** and ^{ns} – indicate significance at $p \leq 0.01$ and not significant, respectively, according to the F-test; CV – coefficient of variation. Lowercase letters differ in electrical conductivity levels of irrigation water (ECw), and uppercase letters differ in melatonin concentrations (MEL) according to Tukey’s test ($p \leq 0.05$). Vertical bars show the means ± standard deviation.

Figure 4. Initial fluorescence – Fo’ (A), maximum fluorescence – Fm’ (B), variable fluorescence – Fv’ (C), basal fluorescence – Fs (D), and ratio between variable and initial

fluorescence – Fv’/Fo’ (E) of soybean plants subjected to different electrical conductivity levels of irrigation water and exogenous application of melatonin.

The ECw significantly influenced the potential quantum yield of the PSII (Fv’/Fm’) (Figure 5A), the effective quantum efficiency of the PSII (ΦPSII) (Figure 5B), non-photochemical dissipation (qN) (Figure 5D), and electron transport rate (ETR) (Figure 5E). In contrast, exogenous melatonin application did not significantly affect any of these parameters, and photochemical dissipation (qP) did not differ significantly between treatments (Figure 5C). Variables Fv’/Fm’, ΦPSII, qN, and ETR decreased under saline conditions (ECw 3.0 and 5.0 dS m^{-1}), showing average reductions of 25.51, 35.37, 13.64, and 35.48%, respectively, when compared to non-saline conditions (ECw 0.5 dS m^{-1}).

The interaction between ECw and exogenous melatonin concentration significantly affected both proline (Figure 5F) and total soluble sugars (TSS) (Figure 5G). For proline, under non-saline conditions (ECw 0.5 dS m^{-1}), the application of 1 mM melatonin increased its content by 65.97% compared to 0 mM. However, under saline conditions at 3.0 dS m^{-1}, the 1 mM melatonin concentration reduced proline accumulation by 36.53% compared to plants without melatonin. In contrast, at 5.0 dS m^{-1}, proline content remained relatively stable across melatonin concentrations. Regarding TSS, the 1 mM melatonin concentration promoted substantial increases of 77.77 and 223.40% under ECw levels of 0.5 and 3.0 dS m^{-1}, respectively, when compared to the 0 mM concentration. Conversely, under severe salt stress (ECw 5.0 dS m^{-1}), melatonin did not enhance TSS accumulation, with a 28.22% decrease at 1 mM compared to the 0 mM control.

The sum of the principal components (PC) showed a total inertia of 89.33% of the total variation (Figure 6). PC1 contributed 74.32% of the total variation and showed positive correlations with the fluorescence variables of chlorophyll a, A, gs, E, Ci, Ci/Ca, and TSS; conversely, it obtained negative correlations with VPD and proline. Proline and VPD showed contrary behavior to the variables, especially for gas exchange (A, gs, and E), showing that the increase in proline is due to the reduction of these variables. It is also noted that the ECw levels of 0.5 dS m^{-1} (0, 0.5, and 1.0 mM) and 3.0 dS m^{-1} (0.5 and 1.0 mM) correlated positively in PC1. PC2 obtained 15.01% of the total variation, showing little influence for the variables analyzed.

Variable A showed positive and very strong correlations with gs (0.92), E (0.91), Fv’ (0.91), Fv’/Fo’ (0.91), ΦPSII (0.91), qN (0.91), and ETR (0.91), and moderate and very strong negative correlations with VPD (-0.46) and proline (-0.91), respectively (Figure 7). On the other hand, VPD showed moderate negative correlations with A (-0.46), gs (-0.52), and E (-0.52), while proline showed strong negative correlations (-0.91), (-0.95), and (0.95) for the same variables, respectively.

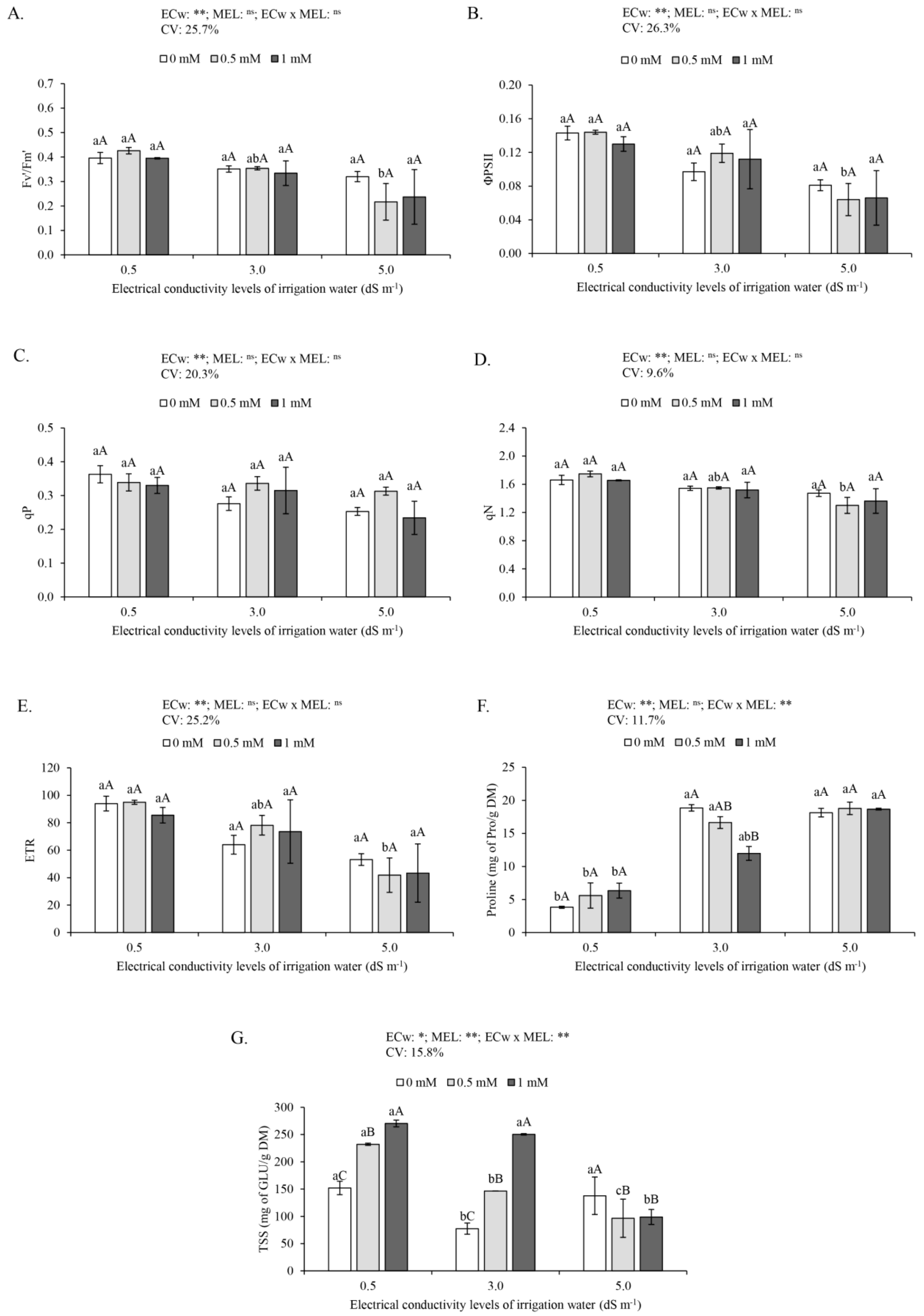

**, *, and ^{ns} – indicate significance at $p \leq 0.01$, $p \leq 0.05$, and not significant, respectively, according to the F-test; CV – coefficient of variation. Lowercase letters differ in electrical conductivity levels of irrigation water (ECw), and uppercase letters differ in melatonin concentrations (MEL) according to Tukey's test ($p \leq 0.05$). Vertical bars show the means ± standard deviation.

Figure 5. Potential quantum yield of PSII – Fv’/Fm’ (A), effective quantum efficiency of PSII – ΦPSII (B), photochemical dissipation – qP (C), non-photochemical dissipation – qN (D), electron transport rate – ETR (E), proline content (F), and total soluble sugars – TSS (G) of soybean plants subjected to different electrical conductivity levels of irrigation water and exogenous melatonin application.

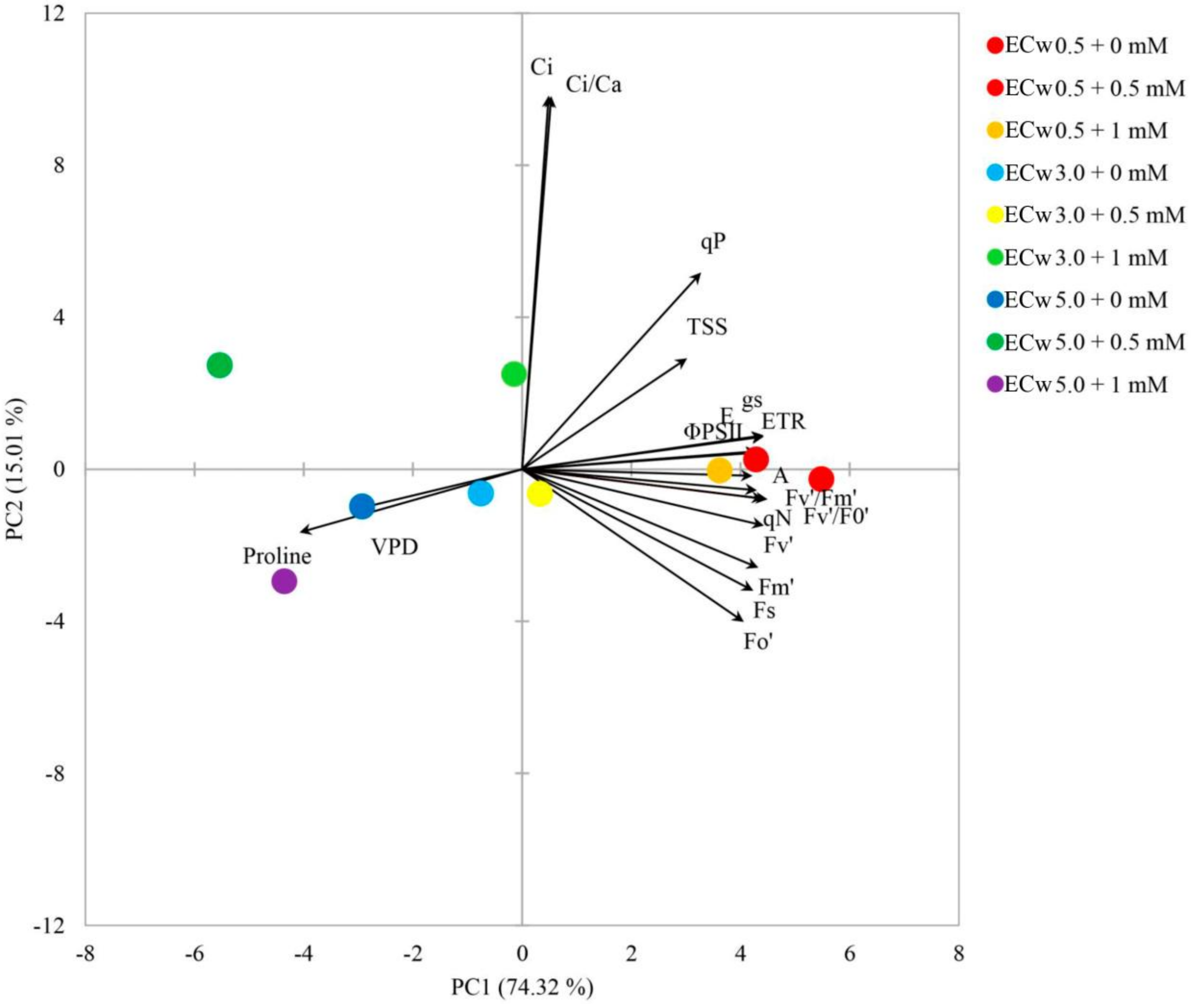

Figure 6. Principal component analysis (PCA) of the variables of physiological and biochemical aspects of soybean plants subjected to different electrical conductivity levels of irrigation water (ECw) and exogenous application of melatonin. A – net CO_2 assimilation rate; gs – stomatal conductance; E – transpiration rate; Ci – internal CO_2 concentration; Ci/Ca – ratio of internal to ambient CO_2 concentration; VPD – vapor pressure deficit; Fo’ – initial fluorescence; Fm’ – maximum fluorescence; Fv’ – variable fluorescence; Fs – basal fluorescence; Fv’/Fo’ – ratio between variable and initial fluorescence; Fv’/Fm’ – potential quantum yield of the PSII; ΦPSII – effective quantum efficiency of the PSII; qP – photochemical dissipation; qN – non-photochemical dissipation; ETR – electron transport rate; TSS – total soluble sugars.

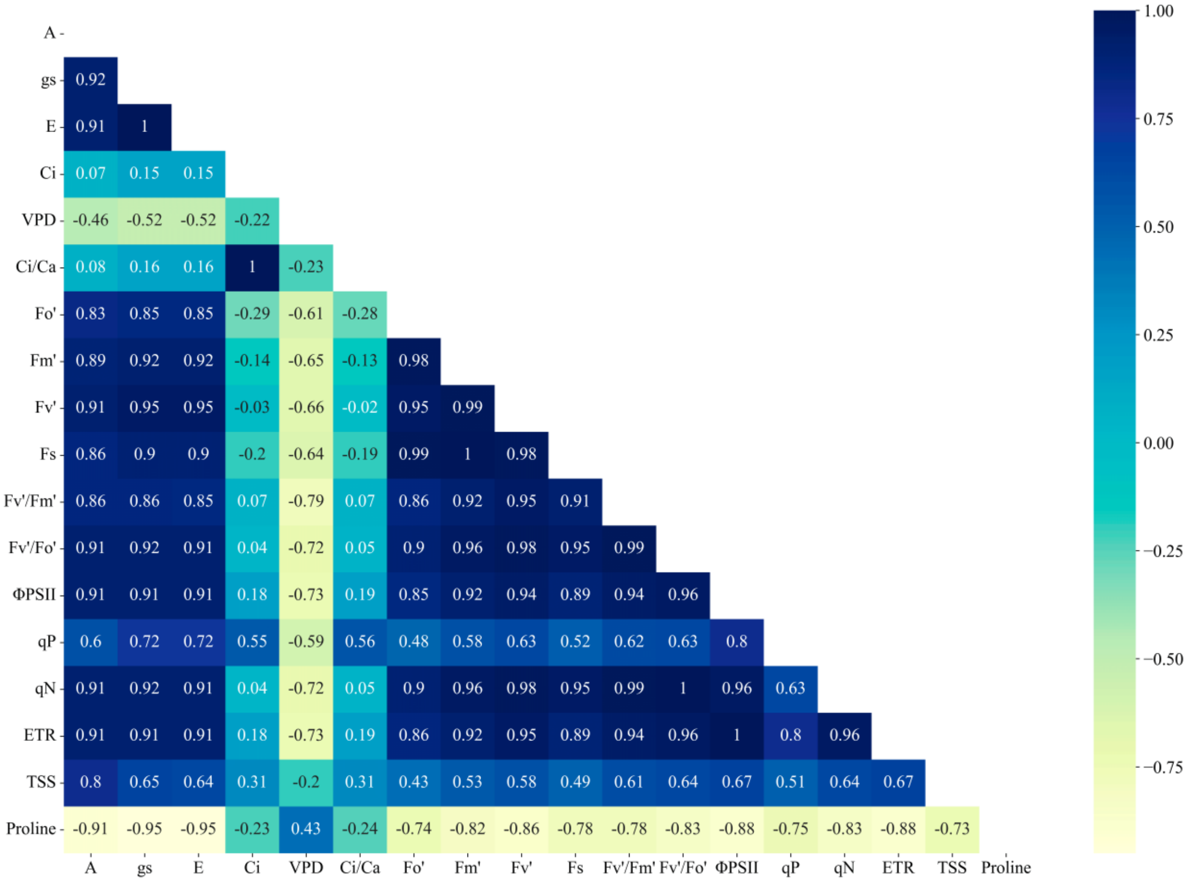

	A	gs	E	Ci	VPD	Ci/Ca	Fo'	Fm'	Fv'	Fs	Fv'/Fm'	Fv'/Fo'	ΦPSII	qP	qN	ETR	TSS	Proline
A																		
gs	0.92																	
E	0.91	1																
Ci	0.07	0.15	0.15															
VPD	-0.46	-0.52	-0.52	-0.22														
Ci/Ca	0.08	0.16	0.16	1	-0.23													
Fo'	0.83	0.85	0.85	-0.29	-0.61	-0.28												
Fm'	0.89	0.92	0.92	-0.14	-0.65	-0.13	0.98											
Fv'	0.91	0.95	0.95	-0.03	-0.66	-0.02	0.95	0.99										
Fs	0.86	0.9	0.9	-0.2	-0.64	-0.19	0.99	1	0.98									
Fv'/Fm'	0.86	0.86	0.85	0.07	-0.79	0.07	0.86	0.92	0.95	0.91								
Fv'/Fo'	0.91	0.92	0.91	0.04	-0.72	0.05	0.9	0.96	0.98	0.95	0.99							
ΦPSII	0.91	0.91	0.91	0.18	-0.73	0.19	0.85	0.92	0.94	0.89	0.94	0.96						
qP	0.6	0.72	0.72	0.55	-0.59	0.56	0.48	0.58	0.63	0.52	0.62	0.63	0.8					
qN	0.91	0.92	0.91	0.04	-0.72	0.05	0.9	0.96	0.98	0.95	0.99	1	0.96	0.63				
ETR	0.91	0.91	0.91	0.18	-0.73	0.19	0.86	0.92	0.95	0.89	0.94	0.96	1	0.8	0.96			
TSS	0.8	0.65	0.64	0.31	-0.2	0.31	0.43	0.53	0.58	0.49	0.61	0.64	0.67	0.51	0.64	0.67		
Proline	-0.91	-0.95	-0.95	-0.23	0.43	-0.24	-0.74	-0.82	-0.86	-0.78	-0.78	-0.83	-0.88	-0.75	-0.83	-0.88	-0.73	

Figure 7. Pearson's correlation of the variables of physiological and biochemical aspects of soybean plants subjected to different electrical conductivity levels of irrigation water (ECw) and exogenous application of melatonin. A – net CO_2 assimilation rate; gs – stomatal conductance; E – transpiration rate; Ci – internal CO_2 concentration; Ci/Ca – ratio of internal to ambient CO_2 concentration; VPD – vapor pressure deficit; Fo' – initial fluorescence; Fm' – maximum fluorescence; Fv' – variable fluorescence; Fs – basal fluorescence; Fv'/Fo' – ratio between variable and initial fluorescence; Fv'/Fm' – potential quantum yield of the PSII; ΦPSII – effective quantum efficiency of the PSII; qP – photochemical dissipation; qN – non-photochemical dissipation; ETR – electron transport rate; TSS – total soluble sugars.

Discussion

The profound impact of salt stress on the physiological and biochemical aspects of soybean crops cannot be overstated. It is a significant environmental factor that impedes plant development (Calzada et al., 2022). The alteration of plant metabolism under salt stress, and the potential intensification of these changes depending on salt concentration and type, are key areas of study (Giordano et al., 2021; Joshi et al., 2022). Metabolic alterations were observed in the present study, indicating that soybean plants are susceptible to increasing salinity.

Our study reveals that the variables A (Figure 2A), gs (Figure 2B), E (Figure 2C), Ci (Figure 3A), and Ci/Ca (Figure 3B) decrease with the increase in salt levels, underscoring the urgent need to address salt stress in soybean crops. This behavior is a direct result of salinity's impact on the soil solution's osmotic potential, which limits water availability and compromises root water absorption (Veloso et al., 2022). The subsequent closure of stomata, reduced CO_2 availability, and decreased transpiration negatively impact photosynthetic rate due to changes in leaf biochemistry (Hamani et al., 2020).

Another significant observation is the increase in VPD as saline levels intensify (Figure 3C). Understanding this variable is crucial for crop development, as increased evaporative demand can be detrimental to plant growth (Shibuya et al., 2018). Under conditions of high evaporation, the sensitivity of guard cells leads to stomatal closure, resulting in a decrease in photosynthetic rate (Jiao et al., 2019). Moreover, in drier regions, the negative impact on photosynthesis is exacerbated by higher VPD (Rigden et al., 2020).

The fluorescence variables of chlorophyll a (Figures 4A-E, 5A, 5B, 5D, and 5E), except for qP (Figure 5C), decreased under saline conditions (ECw 3.0 and 5.0 dS m^{-1}). These results demonstrate that this decline is due to the induced destruction of biosynthetic pathways, as when they are stressed, these photosynthetic pigments degrade, impairing their formation (Alemu, 2020). Thus, evaluating chlorophyll fluorescence has been considered a good indicator of photosynthesis reactions at photosystem II (PSII) (Najar et al., 2019). Among the fluorescence variables, the Fv'/Fm' ratio is widely used because reductions in this ratio indicate PSII inefficiency (Guidi et al., 2019). Thus, the imbalance caused by photochemical activity in PSII reduces ETR by interrupting electron emission. Thus, excess energy excitation favors photoinhibition (Shin et al., 2020). These results reinforce the deleterious effects of salinity, showing that salt stress impairs chlorophyll fluorescence and thereby compromises the photochemical performance of soybean plants (Luo et al., 2021; Deng et al., 2024).

In addition, under salt stress conditions, plants can overcome these adversities through tolerance mechanisms, such as regulation of antioxidant defense, ionic exclusion, and accumulation of osmolytes and secondary metabolites (Calzada et al., 2022). In response to this condition, the interaction between ECw levels and melatonin significantly altered osmolyte accumulation. Notably, proline (Figure 5F) and total soluble sugars (TSS) (Figure 5G) contents were strongly modulated by melatonin under different stress levels. This can be justified because, under salt stress, the content of proline and sugars increases in plants to reestablish osmotic and water balance, a good indicator of plant tolerance (Behdad et al., 2021). Specifically, the exogenous application of 1 mM melatonin boosted both proline and TSS contents under non-saline conditions, and stimulated massive TSS accumulation under moderate salinity (ECw 3.0 dS m^{-1}). This indicates that exogenous melatonin acts proactively to enhance the plant's biochemical osmoprotective reserves. However, under severe salt stress (ECw 5.0 dS m^{-1}), this up-regulation was compromised, suggesting that severe ionic toxicity may overwhelm the protective metabolic pathways mediated by melatonin. It is worth noting that proline, a compatible solute, helps maintain membrane integrity and high turgor pressure, and detoxifies reactive oxygen species (ROS) (Shin et al., 2020).

In addition, the research results showed that Ci (Figure 3A) and Ci/Ca (Figure 3B) were positively influenced by melatonin, while VPD (Figure 3C) was negatively influenced. In summary, it is well established that melatonin plays a crucial role in regulating several key physiological processes in plants, including photosynthesis and osmotic balance, and acts as an antioxidant against reactive oxygen species (ROS) under various abiotic stress conditions (Gul et al., 2021). One explanation that justifies the absence of significant melatonin effects on the gas exchange and chlorophyll fluorescence variables is that melatonin can act in a redox network and initiate signaling processes as a response to stress or else act to improve tolerance through the expression of genes related to cell division, photosynthesis, as well as carbohydrate metabolism to favor plant growth (Wang et al., 2023). Thus, rather than being translocated to protective mechanisms, melatonin may have been redirected to signaling pathways, leading the plant to express delayed stress responses.

It is worth mentioning that the chlorophyll fluorescence parameters are strongly associated with the CO_2 assimilation rate, since an increase in these variables indicates that the PSII reaction center is enhanced, resulting in increments in the photosynthetic rate and accumulation of photoassimilates, as PSII is absorbing, transferring, and converting light energy more efficiently (Rousseau et al., 2013; Shih et al., 2019; Ruiqi et al., 2025). This behavior explains the Pearson correlation results, which show that the CO_2 assimilation rate is strongly positively correlated with Fv', Fv'/Fo', ΦPSII, qN, and ETR (Figure 7). Furthermore, proline content showed negative correlations with CO_2 assimilation rate, stomatal conductance, and transpiration, which is justifiable since proline accumulation is an indicator of stress (Hnilickova et al., 2021), but also plays an essential role in osmoregulation, water retention, reduction of plant cell water potential, and in stabilizing pressure to benefit leaf cell expansion (Dubrovna et al., 2022; Lin et al., 2024).

Conclusions

The electrical conductivity levels of irrigation water of 3.0 and 5.0 dS m^{-1} alter gas exchange, chlorophyll *a* fluorescence, and proline and total soluble sugar contents in soybean plants.

Chlorophyll *a* fluorescence in soybean plants cv. Sambaíba Conventional is not significantly affected by salinity at the level of 3.0 dS m^{-1} when compared to non-saline conditions.

The exogenous application of melatonin mitigates the negative effects of salt stress on internal CO_2 concentration (Ci) and the ratio of intercellular to atmospheric CO_2 (Ci/Ca).

Furthermore, melatonin modulates the accumulation of osmolytes such as proline and total soluble sugars, promoting the maintenance of physiological and biochemical processes. Thus, melatonin shows great potential as a biostimulant to enhance photosynthetic and osmoprotective efficiency, mitigating the deleterious effects of salinity in soybean crops.

References

Alemu, S. T. Photosynthesis limiting stresses under climate change scenarios and role of chlorophyll fluorescence: A review article. Cogent Food & Agriculture, v. 6, n. 1, 1785136, 2020. https://doi.org/10.1080/23311932.2020.1785136

Alvares, C. A.; Stape, J. L.; Sentelhas, P. C.; Gonçalves, J. L. M.; Sparovek, G. Köppen's climate classification map for Brazil. Meteorologische Zeitschrift, v. 22, n. 6, p. 711-728, 2013. https://doi.org/10.1127/0941-2948/2013/0507

Arif, Y.; Singh, P.; Siddiqui, H.; Bajguz, A.; Hayat, S. Salinity induced physiological and biochemical changes in plants: An omic approach towards salt stress tolerance. Plant Physiology and Biochemistry, v. 156, p. 64-77, 2020. https://doi.org/10.1016/j.plaphy.2020.08.042

Atta, K.; Mondal, S.; Gorai, S.; Singh, A. P.; Kumari, A.; Ghosh, T.; Roy, A.; Hembram, S.; Gaikwad, D. J.; Mondal, S.; Bhattacharya, S.; Jha, U. C.; Jespersen, D. Impacts of salinity stress on crop plants: Improving salt tolerance through genetic and molecular dissection. Frontiers in Plant Science, v. 14, 1241736, 2023. https://doi.org/10.3389/fpls.2023.1241736

Bates, L. S.; Waldren, R. P. A.; Teare, I. D. Rapid determination of free proline for water-stress studies. Plant and Soil, v. 39, n. 1, p. 205-207, 1973. https://doi.org/10.1007/BF00018060

Behdad, A.; Mohsenzadeh, S.; Azizi, M. Growth, leaf gas exchange and physiological parameters of two *Glycyrrhiza glabra* L. populations subjected to salt stress condition. Rhizosphere, v. 17, 100319, 2021. https://doi.org/10.1016/j.rhisph.2021.100319

Calzada, K. P.; Viciedo, D. L.; Habermann, E.; Hurtado, A. C.; Gratão, P. L.; Prado, R. M.; Lata-Tenesaca, L. F.; Martinez, C. A.; Celi, G. E. A.; Rodríguez, J. C. Exogenous application of amino acids mitigates the deleterious effects of salt stress on soybean plants. Agronomy, v. 12, n. 9, 2014, 2022. https://doi.org/10.3390/agronomy12092014

Coêlho, E. S.; Ribeiro, J. E. S.; Oliveira, P. H. A.; Silva, E. F.; Silva, A. G. C.; Oliveira, A. K. S.; Santos, G. L.; Silva, T. I.; Rodriguez, R. M.; Bezerra, A. L.; Barros Júnior, A. P.; Silveira, L. M. Application of biostimulants modulates photosynthesis responses, and chlorophyll fluorescence under salt stress in radish. Journal of Plant Growth Regulation, v. 44, n. 9, p. 5063-5078, 2025. https://doi.org/10.1007/s00344-025-11735-2

Corwin, D. L. Climate change impacts on soil salinity in agricultural areas. European Journal of Soil Science, v. 72, n. 2, p. 842-862, 2021. https://doi.org/10.1111/ejss.13010

Cotrim, M. F.; Gava, R.; Campos, C. N. S.; David, C. H. O.; Reis, I. D. A.; Teodoro, L. P. R.; Teodoro, P. E. Physiological performance of soybean genotypes grown under irrigated and rainfed conditions. Journal of Agronomy and Crop Science, v. 207, n. 1, p. 34-43, 2021. https://doi.org/10.1111/jac.12448

Deng, Y.; Xin, N.; Zhao, L.; Shi, H.; Deng, L.; Han, Z.; Wu, G. Precision detection of salt stress in soybean seedlings based on deep learning and chlorophyll fluorescence imaging. Plants, v. 13, n. 15, 2089, 2024. https://doi.org/10.3390/plants13152089

DuBois, M.; Gilles, K. A.; Hamilton, J. K.; Rebers, P. A; Smith, F. Colorimetric method for determination of sugars and related substances. Analytical Chemistry, v. 28, n. 3, p. 350-356, 1956. https://doi.org/10.1021/ac60111a017

Dubrovna, O. V.; Mykhalska, S. I.; Komisarenko, A. G. Using proline metabolism genes in plant genetic engineering. Cytology and Genetics, v. 56, n. 4, p. 361-378, 2022. https://doi.org/10.3103/S009545272204003X

Eswar, D.; Karuppusamy, R.; Chellamuthu, S. Drivers of soil salinity and their correlation with climate change. Current Opinion in Environmental Sustainability, v. 50, p. 310-318, 2021. https://doi.org/10.1016/j.cosust.2020.10.015

Ferreira, D. F. Sisvar: A guide for its Bootstrap procedures in multiple comparisons. Ciência e Agrotecnologia, v. 38, n. 2, p. 109-112, 2014. https://doi.org/10.1590/S1413-70542014000200001

Ferreira, T. R.; Maguire, M. S.; Silva, B. B.; Neale, C. M. U.; Serrão, E. A. O.; Ferreira, J. D.; Moura, M. S. B.; Santos, C. A. C; Silva, M. T.; Rodrigues, L. N.; Carvalho, H. F. S. Assessment of water demands for irrigation using energy balance and satellite data fusion models in cloud computing: A study in the Brazilian semiarid region. Agricultural Water Management, v. 281, 108260, 2023. https://doi.org/10.1016/j.agwat.2023.108260

Giordano, M.; Petropoulos, S. A.; Rouphael, Y. Response and defence mechanisms of vegetable crops against drought, heat and salinity stress. Agriculture, v. 11, n. 5, 463, 2021. https://doi.org/10.3390/agriculture11050463

Girardi, L. B.; Peiter, M. X.; Bellé, R. A.; Robaina, A. D.; Torres, R. R.; Kirchner, J. H.; Ben, L. H. B. Evapotranspiração e coeficiente de cultura da alstroemeria (*Alstroemeria x hybrida*) cultivada em estufa. Irriga, v. 21, n. 4, p. 817-829, 2016. https://doi.org/10.15809/irriga.2016v21n4p817-829

Gomes, R. V.; Coutinho, G. V. Recomendações de calcário e fertilizantes: Soja *Glycine max* (L.) Merr. In: Cavalcanti, F. J. A.; Santos, J. C. P.; Pereira, J. R.; Leite, J. P.; Silva, M. C. L.; Freire, F. J.; Silva, D. J.; Sousa, A. R.; Messias, A. S.; Faria, C. M. B.; Burgos, N.; Lima Júnior, M. A.; Gomes, R. V.; Cavalcanti, A. C.; Lima, J. F. W. F. (Coord.). Recomendações de adubação para o estado de Pernambuco: 2ª aproximação. 3.ed. Recife: Instituto Agronômico de Pernambuco, 2008. p. 190.

Guidi, L.; Lo Piccolo, E.; Landi, M. Chlorophyll fluorescence, photoinhibition and abiotic stress: Does it make any difference the fact to be a C3 or C4 species? Frontiers in Plant Science, v. 10, 174, 2019. https://doi.org/10.3389/fpls.2019.00174

Gul, M.; Khan, F. A.; Wani, S. A.; Bhat, S. A.; Mir, S. A.; Malik, A.; Kumar, A.; Narayan, S.; Moinuddin.; Fayaz, F.; Lone, S. A. Effects of foliar application of melatonin on gas exchange and certain biochemical characteristics broccoli cv. Palam Samridhi. Journal of Applied and Natural Science, v. 13, n. 2, p. 791-797, 2021. https://doi.org/10.31018/jans.v13i2.2673

Hailu, B.; Mehari, H. Impacts of soil salinity/sodicity on soil-water relations and plant growth in dry land areas: A review. Journal of Natural Sciences Research, v. 12, n. 3, p. 1-10, 2021. https://doi.org/10.7176/JNSR/12-3-01

Hamani, A. K. M.; Wang, G.; Soothar, M. K.; Shen, X.; Gao, Y.; Qiu, R.; Mehmood, F. Responses of leaf gas exchange attributes, photosynthetic pigments and antioxidant enzymes in NaCl-stressed cotton (*Gossypium hirsutum* L.) seedlings to exogenous glycine betaine and salicylic acid. BMC Plant Biology, v. 20, n. 1, 434, 2020. https://doi.org/10.1186/s12870-020-02624-9

Jahan, M. S.; Zhao, C. J.; Shi, L. B.; Liang, X. R.; Jabborova, D.; Nasar, J.; Zhou, X. B. Physiological mechanism of melatonin attenuating to osmotic stress tolerance in soybean seedlings. Frontiers in Plant Science, v. 14, 1193666, 2023. https://doi.org/10.3389/fpls.2023.1193666

Hnilickova, H.; Kraus, K.; Vachova, P.; Hnilicka, F. Salinity stress affects photosynthesis, malondialdehyde formation, and proline content in *Portulaca oleracea* L. Plants, v. 10, n. 5, 845, 2021. https://doi.org/10.3390/plants10050845

Jiao, X. C.; Song, X. M.; Zhang, D. L.; Du, Q. J.; Li, J. M. Coordination between vapor pressure deficit and CO_2 on the regulation of photosynthesis and productivity in greenhouse tomato production. Scientific Reports, v. 9, n. 1, 8700, 2019. https://doi.org/10.1038/s41598-019-45232-w

Joshi, S.; Nath, J.; Singh, A. K.; Pareek, A.; Joshi, R. Ion transporters and their regulatory signal transduction mechanisms for salinity tolerance in plants. Physiologia Plantarum, v. 174, n. 3, e13702, 2022. https://doi.org/10.1111/ppl.13702

Lin, S.; Zhang, W.; Wang, G.; Hu, Y.; Zhong, X.; Tang, G. Physiological regulation of photosynthetic-related indices, antioxidant defense, and proline anabolism on drought tolerance of wild soybean (*Glycine soja* L.). Plants, v. 13, n. 6, 880, 2024. https://doi.org/10.3390/plants13060880

Luo, B.; Wang, C.; Wang, X.; Zhang, H.; Zhou, Y.; Wang, W.; Song, P. Changes in photosynthesis and chlorophyll fluorescence in two soybean (*Glycine max*) varieties under NaCl stress. International Journal of Agricultural and Biological Engineering, v. 14, n. 3, p. 76-82, 2021. https://doi.org/10.25165/j.ijabe.20211403.5941

Muhammad, M.; Waheed, A.; Wahab, A.; Majeed, M.; Nazim, M.; Liu, Y. H.; Li, W. J. Soil salinity and drought tolerance: An evaluation of plant growth, productivity, microbial diversity, and amelioration strategies. Plant Stress, v. 11, 100319, 2023. https://doi.org/10.1016/j.stress.2023.100319

Najar, R.; Aydi, S.; Sassi-Aydi, S.; Zarai, A.; Abdelly, C. Effect of salt stress on photosynthesis and chlorophyll fluorescence in *Medicago truncatula*. Plant Biosystems - An International Journal Dealing with all Aspects of Plant Biology, v. 153, n. 1, p. 88-97, 2019. https://doi.org/10.1080/11263504.2018.1461701

Oliveira, P. H. A.; Sá, S. A.; Ribeiro, J. E. S.; Silva, J. P. P.; Lima, F. F.; Silva, I. B. M.; Silveira, L. M.; Barros Júnior, A. P. Exogenous application of melatonin mitigates salt stress in soybean. Revista Caatinga, v. 38, e12698, 2024. https://doi.org/10.1590/1983-21252025v3812698rc

Pan, Y.; Xu, X.; Li, L.; Sun, Q.; Wang, Q.; Huang, H.; Tong, Z.; Zhang, J. Melatonin-mediated development and abiotic stress tolerance in plants. Frontiers in Plant Science, v. 14, 1100827, 2023. https://doi.org/10.3389/fpls.2023.1100827

R Core Team. R: A language and environment for statistical computing. R Foundation for Statistical Computing, 2023. Available on: <https://www.r-project.org/>. Accessed on: 06/10/2024.

Raza, A.; Mubarik, M. S.; Sharif, R.; Habib, M.; Jabeen, W.; Zhang, C.; Chen, H.; Chen, Z. H.; Siddique, K. H. M.; Zhuang, W.; Varshney, R. K. Developing drought-smart, ready-to-grow future crops. The Plant Genome, v. 16, n. 1, e20279, 2023. https://doi.org/10.1002/tpg2.20279

Ribeiro, J. E. S.; Silva, A. G. C.; Coêlho, E. S.; Oliveira, P. H. A.; Silva, E. F.; Oliveira, A. K. S.; Barros Júnior, A. P. Melatonin mitigates salt stress effects on the growth and production aspects of radish. Revista Brasileira de Engenharia Agrícola e Ambiental, v. 28, n. 4, e279006, 2024. https://doi.org/10.1590/1807-1929/agriambi.v28n4e279006

Richards, L. A. Diagnosis and improvement of saline and alkaline soils. Washington: United States Salinity Laboratory Staff, 1954. 160p.

Rigden, A. J.; Mueller, N. V.; Holbrook, N. M.; Pillai, N.; Huybers, P. Combined influence of soil moisture and atmospheric evaporative demand is important for accurately predicting US maize yields. Nature Food, v. 1, n. 2, p. 127-133, 2020. https://doi.org/10.1038/s43016-020-0028-7

Rousseau, C.; Belin, E.; Bove, E.; Rousseau, D.; Fabre, F.; Berruyer, R.; Guillaumès, J.; Manceau, C.; Jacques, M. A.; Boureau, T. High throughput quantitative phenotyping of plant resistance using chlorophyll fluorescence image analysis. Plant Methods, v. 9, n. 1, 17, 2013. https://doi.org/10.1186/1746-4811-9-17

Ruiqi, F.; Weiyu, W.; Yanli, D.; Junjie, X.; Liang, C.; Changjun, Z.; Qiang, Z.; Yuxian, Z. Exogenous melatonin increased soybean yield under saline-alkali stress by enhancing plant carbohydrate metabolism and transportation. Physiologia Plantarum, v. 177, n. 4, e70378, 2025. https://doi.org/10.1111/ppl.70378

Sharmin, R. A.; Bhuiyan, M. R.; Lv, W.; Yu, Z.; Chang, F.; Kong, J.; Bhat, J. A.; Zhao, T. RNA-Seq based transcriptomic analysis revealed genes associated with seed-flooding tolerance in wild soybean (*Glycine soja* Sieb. & Zucc.). Environmental and Experimental Botany, v. 171, 103906, 2020. https://doi.org/10.1016/j.envexpbot.2019.103906

Shibuya, T.; Kano, K.; Endo, R.; Kitaya, Y. Effects of the interaction between vapor-pressure deficit and salinity on growth and photosynthesis of *Cucumis sativus* seedlings under different CO_2 concentrations. Photosynthetica, v. 56, n. 3, p. 893-900, 2018. https://doi.org/10.1007/s11099-017-0746-8

Shih, T. H.; Lin, S. H.; Huang, M. Y.; Huang, W. D.; Yang, C. M. Transcriptome profile of the variegated *Ficus microcarpa* cv milky stripe fig leaf. International Journal of Molecular Sciences, v. 20, n. 6, 1338, 2019. https://doi.org/10.3390/ijms20061338

Shin, Y. K.; Bhandari, S. R.; Jo, J. S.; Song, J. W.; Cho, M. C.; Yang, E. Y.; Lee, J. G. Response to salt stress in lettuce: Changes in chlorophyll fluorescence parameters, phytochemical contents, and antioxidant activities. Agronomy, v. 10, n. 11, 1627, 2020. https://doi.org/10.3390/agronomy10111627

Stavi, I.; Thevs, N.; Priori, S. Soil salinity and sodicity in drylands: A review of causes, effects, monitoring, and restoration measures. Frontiers in Environmental Science, v. 9, 712831, 2021. https://doi.org/10.3389/fenvs.2021.712831

Stefanov, M. A.; Rashkov, G. D.; Borisova, P. B.; Apostolova, E. L. Changes in photosystem II complex and physiological activities in pea and maize plants in response to salt stress. Plants, v. 13, n. 7, 1025, 2024. https://doi.org/10.3390/plants13071025

Veloso, L. L. S. A.; Silva, A. A. R.; Lima, G. S.; Azevedo, C. A. V.; Gheyi, H. R.; Moreira, R. C. L. Growth and gas exchange of soursop under salt stress and hydrogen peroxide application. Revista Brasileira de Engenharia Agrícola e Ambiental, v. 26, n. 2, p. 119-125, 2022. https://doi.org/10.1590/1807-1929/agriambi.v26n2p119-125

Wang, Q.; Liang, X.; Xiang, D.; Xu, W.; Wang, C.; Zhan, C.; Ren, C.; Wei, L.; Zhang, S.; Zhang, L.; Wang, J.; Gui, L. The physiological mechanism of melatonin enhancing the tolerance of oat seedlings under saline–alkali stress. Agronomy, v. 13, n. 9, 2343, 2023. https://doi.org/10.3390/agronomy13092343

Yildiz, M.; Poyraz, I.; Çavdar, A.; Özgen, Y.; Beyaz, R. Plant responses to salt stress. In: Ibrokhim Y. A. (ed.). Plant breeding-current and future views. London: IntechOpen, 2020. p. 143-161. https://doi.org/10.5772/intechopen.91551

Zhao, J.; Wang, C.; Shi, X.; Bo, X.; Li, S.; Shang, M.; Chen, F.; Chu, Q. Modeling climatically suitable areas for soybean and their shifts across China. Agricultural Systems, v. 192, 103205, 2021. https://doi.org/10.1016/j.agsy.2021.103205